Spectroscopic evidences for intermediate species formed during aniline polymerization and polyaniline degradation

G.A. Planes[a,b], J.L. Rodríguez[a], M.C. Miras[b], E. Pastor*[a] and C.A. Barbero *[b]

Received (in XXX, XXX) 1st January 2008, Accepted 1st January 2008
First published on the web 1st January 2008
DOI: 10.1039/b000000x

Spectroscopic methods are used to investigate the formation of low molecular mass intermediates during aniline (ANI) oxidation and polyaniline (PANI) degradation. Studying ANI anodic oxidation by in-situ Fourier transform infrared spectroscopy (FTIRS) it is possible to obtain, for the first time, spectroscopic evidences for ANI dimers produced by head-to-tail (4-aminodiphenylamine, 4ADA) and tail-to-tail (benzidine, BZ) coupling of ANI cation radicals. The 4ADA dimer is adsorbed on the electrode surface during polymerization, as proved by cyclic voltammetry of thin PANI films and its infrared spectrum. This method also allows, with the help of computal simulations, assigning characteristic vibration frequencies for the different oxidation states of PANI. The presence of 4ADA retained inside thin polymer layers is established too. On the other hand, FTIRS demonstrates that the electrochemically promoted degradation of PANI renders p-benzoquinone as its main product. This compound, retained inside the film, is apparent in the cyclic voltammogram in the same potential region previously observed for 4ADA dimer. Therefore, applying in-situ FTIRS is possible to distinguish between different chemical species (4ADA or p-benzoquinone) which give rise to voltammetric peaks in the same potential region. Indophenol and CO_2 are also detected by FTIRS during ANI oxidation and polymer degradation. The formation of CO_2 during degradation is confirmed by differential electrochemical mass spectroscopy. In the best of our knowledge, this is the first evidence of the oxidation of a conducting polymer to CO_2 by electrochemical means. The relevance of the production of different intermediate species towards PANI fabrication and applications is discussed.

.

A Introduction

Polyaniline (PANI) is one of the most studied conjugated conducting polymers, due to its interesting properties such as environmental stability, good electrical conductivity, low cost and easy synthesis. [1,2] It is clear that aniline (ANI) polymerization begins by the oxidative formation of ANI radical cations, which then form dimers through follow-up chemical reactions. The nature of those species is relevant both towards PANI synthesis and material properties (conductivity, toxicity, etc.). As it was early pointed out by Adams,[3] both the head-to-tail (4-aminodiphenylamine, 4ADA) and tail-to-tail (benzidine, BZ) ANI dimers could initiate polymerization, and therefore, be included in the polymer structure. Thus it is important to elucidate which of those products are formed in the early stages of polymerization. Moreover, BZ contamination of the polymer should be avoided owing to its well known carcinogenicity. [4] Its retention inside the polymer, production by polymer degradation or formation in the polymerization solution is a concern when practical applications of the polymer are envisaged. [5]

On the other hand, it has been recently shown that mass transport of reactants and products plays a critical role on the aggregation state of the resulting PANI.[6] In that way, it is possible to produce PANI nanofibers or microscopic aggregates by controlling the stirring of the polymerization solution. Moreover, addition of small amount of aromatic diamines,[7] including BZ,[8] strongly influences the polymerization rate and polymer morphology. It is therefore likely that the presence of intermediates produces changes in the polymer morphology and aggregation.

Since it has been shown that ANI chemical[9] and electrochemical [10] polymerizations follow the same kinetic mechanism, data obtained from electrochemical studies could be applied to the chemical polymerization used in industrial PANI production. Indeed, it has been observed that the same factors (anion type, aromatic diamines, etc.) affect in the same way the chemical [11] and electrochemical [12] polymerization.

The electrochemical oxidation of aromatic amines has been extensively studied in the past using voltammetric techniques combined with chemical synthesis of products. [13] The interest in this field has been renewed recently owing to the role of those compounds as monomers of conducting polymers. [14]

ANI electropolymerization begins with monomer oxidation to the corresponding radical cation. The radical cation suffers various follow up chemical reactions, including dimerization and coupling with the parent molecule. By comparison of the cyclic voltammogram (CV) obtained during ANI oxidation in acid media and those of chemically synthesized dimers, Bacon & Adams [15] established that head-to tail (N-C4) (4ADA) and tail-tail (C4-C4') (BZ) dimers are the main products in this oxidation reaction⊗. However, direct spectroscopic evidence for such dimers is rarelly found in the literature[16].

In-situ spectroscopic techniques, such as differential electrochemical mass spectroscopy (DEMS) [17] and Fourier transform infrared spectroscopy (FTIRS), [18] which have been originally applied to analyze the electrochemical behavior of simple organic species, [19] can be extended to more complex compounds [20] . In-situ FTIRS has been used to study the redox processes in PANI, mainly in the internal reflection configuration (attenuated total reflection, ATR) [20-22] and less often by external reflection. [23-25] Dunsch and coworkers used ATR [26] and electron paramagnetic resonance (EPR) [27,28] combined with UV-vis spectroscopy to follow ANI electropolymerization. Nakayama et al investigated PANI formation by time-resolved FTIR under potentiostatic control. [29] In all these studies, only final products (PANI or oligomers) were observed. There is no reported detection of intermediate dimers. Also, in-situ Raman spectroscopy (including surface enhanced resonance spectroscopy (SERS) and resonance Raman) has been extensively employed with this purpose. [30-35]

On the other hand, few applications of in-situ techniques have been reported for the elucidation of ANI electrochemical oxidation process. The adsorption of ANI at Au electrodes was studied by Holze [36] using SERS. Schmiemann et al applied DEMS to study the adsorption and complete oxidation of ANI on Pt. [37] Only the products of the complete oxidation of ANI were detected and no attempt was made to detect intermediate oxidation products or polymer formation. Cases et al studied ANI electrochemical oxidation [38] at pH 5, where only the head-to-tail dimer (4ADA) was detected by in-situ FTIR. However, they found that the oxidation of the dimer in the same media gives a conducting polymer different to PANI. [39]

Besides identifying the dimers produced during the initial stages of ANI polymerization, it is important to ascertain the nature of features present in the voltammetric profiles. While PANI displays two main redox systems, corresponding to the conversion of leucoemeraldine to emeraldine and subsequent conversion of the later to pernigraniline, a third broad "middle peak" could be present, depending on the preparation conditions. In addition, a similar "middle peak" arises when the polymer is degraded by subjecting it to extreme anodic potentials in aqueous media. [40] The "middle peak" feature has been assigned to the redox reaction of hydrolysis products (quinone/hydroquinone), [41] dimers or crosslinked units [42]. Furthermore, recently XPS confirms a considerable amount of quinone/hydroquinone as side product formed in electropolymerized films.[43] However, it was difficult to deduce the effect of the applied potential on the amount of benzoquinone and hidroquinone (by the observation of the C1s) because the energy difference between the different carbon–oxygen bonds was too small to be resolved.Using spectroelectrochemical methods, the nature of the so called "middle peak" in the polymer redox response will be clarified.

The aim of the present work is to detect the species formed during the early stages of ANI polymerization in acid media, which is the most common polymerization condition, and to find the nature of soluble and/or adsorbed intermediates as well as the products of PANI degradation. With this purpose, external reflection in-situ FTIRS and DEMS are used.Computational calculations have been applied to confirm the assignment of IR bands.

B Experimental

PANI was synthesized by scanning the electrode from 0.1 to 1.05 V_{RHE} at 50 mV/s during three cycles in order to initiate the polymerization, and then continuous cycling in the 0.1 – 0.9 V_{RHE} potential range until the desired thickness was achieved, typically 50 cycles. The first three cycles allows to form a polymer layer which catalyzes further polymerization. Then, the potential is reduced to maintain the current density low avoiding complete depletion of aniline from the diffusion layer. If aniline is depleted, the oxidized polymer could react with water, leading to degradation (see below). Three distinctive solutions were employed (0.01 M, 0.05 M and 0.1 M ANI), all them in 1 M perchloric acid.

Aniline (Fluka, analytical) was used as received. All other chemicals were of analytical grade. Solutions were prepared with ultrapure (Millipore) water and degassed by bubbling pure Ar. The electrochemical experiments were controlled by a computerized potentiostat (Heka).

4-aminodiphenylamine and benzidine (Aldrich) were purified by twofold crystallization from absolute ethanol. Electrochemical measurements were performed usimg 10 mM solution of 4ADA or BZ in 1 M $HClO_4$. Dimer adsorption was measured by immersion of the Pt electrode in a 0.1 % solution of the dimer in methanol.

DEMS

The working electrode (electrochemical area ca. 5.5 cm^2), consists of a Pt layer sputtered on a microporous semipermeable membrane (Scimat, average thickness 60 μm, porosity 50 %, mean pore size 0.17 μm). The electrochemical cell was completed with a Pt wire as counter electrode and a reversible hydrogen electrode (RHE) in the same electrolyte as reference electrode. All potentials in the text are referred to this electrode. The DEMS cell is directly attached to the vacuum chamber containing the mass spectrometer (Balzers QMG 112) with a Faraday cup detector. Volatile species generated at the electrode evaporate at the pores of the membrane into the vacuum and are detected by the mass spectrometer with a time constant of ca. 1 s. This time constant is small enough to allow mass spectrometric cyclic voltammograms (MSCVs) for selected mass-to-charge ratios (*m/z*) to be recorded in parallel to cyclic voltammograms

⊗ An additional dimer, hydrazobenzene, due head-to-head (N-N) coupling is only formed at high pH.

(CVs) at a scan rate of 0.01V s^{-1}.

In-situ FTIR spectroscopy

The FTIR spectrometer was a Bruker Vector 22 provided with a mercury-cadmium telluride detector. Parallel (*p*) polarized IR light was employed unless otherwise specified. A glass cell with a 60° CaF_2 prism at its bottom was used. The working electrode was a Pt disk placed on one of the prism faces connected with a Pt wire. The disk was cleaned before each experiment by heating in a gas flame and washed with pure water.

The cell and experimental arrangements were described previously.[44] A sketch of the set-up is depicted in the ESI. The electrochemistry inside the in-situ FTIR cell is made in thin layer conditions, due to the proximity of the electrode towards the window necessary to minimize water IR absorption. Spectra were computed from the average of 128 scans obtained with resolution of 8 cm^{-1} and are presented as the reflectance ratio R/R_0, where R and R_0 are the reflectances measured at the sample and the reference potential, respectively. In this way, bands pointing upward (positive bands) are related to species which are present in a greater amount at the reference potential (consumed), whereas bands pointing downward (negative bands) correspond to species in a greater amount at the sample potential (produced).

Computational simulation of the IR spectra

To help the assignment of IR bands in the spectra to molecular species and/or functional groups, computational simulation of the IR spectra of reactants and products was perfomed using Density Functional Theory (DFT) with a B3LYP/6-31G base. The procedsure involve the following steps:

1) Drawing the structure with charges and anions when necessary using ChemDraw Ultra 11.
2) Minimize the structure using Merck Molecular Force Field 94 (MMFF94) in ChemDraw Bio3D 11.
3) Minimize the Energy/Geometry using PM3 in the GAMESS interface of ChemDraw Bio3D 11.
4) Predict the IR/Raman spectrum using DFT with a B3LYP/6-31G base in the GAMESS interface of ChemDraw Bio3D 11.

In the case of polymeric species a model unit, as described in ESI, was used to allow a reasonable calculation time.

The calculations were made in a Intel Dual Core 2.6 GHz computer with 5 Mb of RAM. The calculated spectral data of each species are shown in the ESI.

C Results and discussion

Aniline oxidation

To be able to study the oxidation of ANI with limited interference of PANI formation, a low concentration of the monomer (10 mM) was used. The cyclic voltammogram during oxidation of ANI in acid media is shown in Figure 1A. The CV is similar to that reported in the literature.[7] In the initial scan, only an oxidation peak at ca. 1.17 VRHE is observed. The absence of the corresponding reduction feature is related to the existence of a fast chemical reaction of the oxidation product with ANI (or dimerization).[8] Indeed, in the backward scan two new quasireversible features are observed at ca. 0.9 and 0.7 V, supporting an ECE (or EC1E1 and EC2E2) mechanism. These contributions are related to the anodic oxidation waves in the second forward scan, indicating that are due to stable products. The peak systems at 0.7 (c-c`) and 0.9 VRHE (b-b`) have been indirectly assigned in the literature, by recording the CV of the mixture of ANI with the pure substances, to the oxidation/reduction of 4ADA and BZ, respectively. BZ is produced by tail to tail coupling (see reaction (2) in Scheme 1) while 4ADA arises from head to tail coupling (see reaction (3) in Scheme 1).[7] The measurement in the backward scan allows clarifying the destiny of all species in the solution.

In-situ FTIR spectra taken while the potential is stepped into the oxidation region and back, with a reference spectrum taken at 0.1 V, are shown in Figure 1B. A positive (consumption) band is observed at 1500 cm^{-1} during the forward scan and assigned to the aromatic C=C stretching of ANI. In the backward scan, a new increasingly negative (production) contribution develops at ca. 1514 cm^{-1}, whereas that at 1500 cm^{-1} seems to decrease. Additional negative signals appear at 1475, 1457, 1323 and 1243 cm^{-1} whereas positive bands are observed at 1551, 1536 and 1293 cm^{-1}.

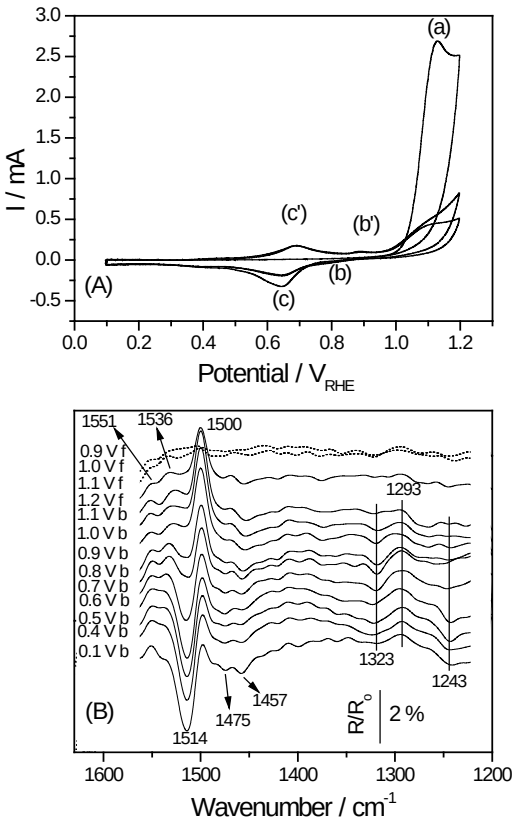

Figure 1. (A) CV for a polycrystalline Pt in a 10 mM solution of ANI in 0.1 M $HClO_4$. Scan rate = 50 mV/s. (B) In-situ FTIR measurements taken during oxidation of ANI (10 mM/0.1 M $HClO_4$) on polycrystalline Pt. Sample potentials as indicated in the figure (f = forward, b = backward step direction). Reference potential = 0.10 V. Spectra taken with p-polarized light, 128 scans at 8 cm^{-1} resolution.

The decrease of the band at 1500 cm^{-1} could be related, in principle with an increase of ANI concentration by reduction of oxidized ANI. However, it has been shown that the follow

up reactions (2) and (3) in Scheme 1 are irreversible and very fast, therefore ANI is not restored by reduction in the back scan. It should be noted that protonated aniline is the dominant species in the acidic condition. However, the deprotonation is faster than the oxidation reaction meaning that there is no kinetic constraint from deprotonation. Only 4ADA and BZ are considered as dimeric products because they are predominant in acid media while hydrazobenzene or azobenzene could appear in neutral or basic media.

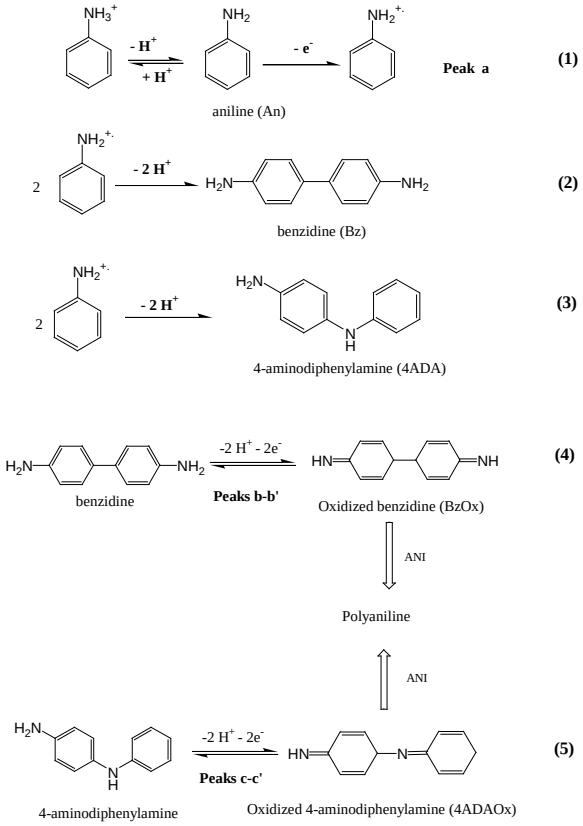

Scheme 1. Mechanism of ANI electrochemical oxidation and dimer formation.

On the other hand, the band at 1514 cm^{-1}, which can be attributed to the aromatic C=C stretching in the reduced dimers, could disturb the positive contribution from ANI at 1500 cm^{-1}. This assignment will be reconsidered later. Excluding the later band, some tentative assignments related to the others signals are described in Table 1 and Scheme 2.

Moreover, two additional bands are observed at 2630 (positive) and 2340 cm^{-1} (negative) (corresponding wavenumber region is not shown in Figure 1B, see Figure S1 in the supplementary information). The latter signal increases monotonically during oxidation, remaining constant during reduction, and it is assigned to CO_2 produced during oxidation of adsorbed ANI.[45] The broad positive band observed at 2630 cm^{-1}, increases during oxidation and decreases during reduction. It is related to the stretching of amino charged species for ANI and the dimers. Upon oxidation, ANI is consumed, and the positive feature increases. During the negative going step scan, the reduced dimers are formed which present a negative band at the same wavenumber region, thus producing a decrease in the total band intensity.

It is tempting to describe the intensity changes of the band at 1500 cm^{-1} during ANI oxidation as changes in molecular orientation and/or adsorption/desorption of ANI or the dimer. To check that possibility, FTIR spectra were taken with s-polarized light (Figure S2, supplementary information). In these spectra, similar behavior is recorded for the signal mentioned before, precluding assignment to adsorbed species. In fact, transmission spectra of protonated 4ADA, BZ and ANI [46] reveal that ANI has a strong absorption band at 1496 cm^{-1}, BZ one at 1501 cm^{-1}, whereas 4ADA shows a contribution at 1516 cm^{-1}.

Table 1. Assignment of vibrational bands observed during ANI oxidation (Figure 1B). The wavenumber values calculated by DFT to the vibrations described in the table are shown between parentheses.[⊗]

Wavenumber/ cm^{-1}	Sense	Vibration	Species
1551 (1582)	+	C=C str.	*ANI* [a]
1536 (1535)	+	NH_2 plane bending	*ANI* [a]
1500	+	C=C aromat. str.	*See text*
1514 (1536)	-	C=C aromat. str.	*4ADA* [b]
1475 (1483)	-	Bending secondary N-H	*4ADA* [a]
1457 (1462)	-	C=C arom. str.	*4ADA* [c] *& BZ* [c]
1323 (1341)	-	C–N str.ar.sec.amines [d]	*4ADA* [b]
1293 (1335)	+	C-N symmetric str.	*ANI* [a]
1243 (1240)	-	C-N str	*4ADA* [c] *& BZ* [c]

[a] *E. Pretsch, P. Bühlmann, C. Affolder,* Structure Determination of Organic Compounds, *Springer, Berlin, 2000.*

[b] *P. Sett, A.K. De, S. Chattopadhyay, P.K. Mallick,* Chemical Physics, *2002*, ***276***, *211-224.*

[c] *S. Akyüz, T. Akyüz, N.M. Ozer,* J. Mol. Struct., *2001*, ***565***, *493-496.*

[d] *R. Buvaneswari, A. Gopalan, T. Vasudevan, H-L. Wang,; T-C. Wen,* Thin Solid Films, *2004*, ***458,*** *77-85.*

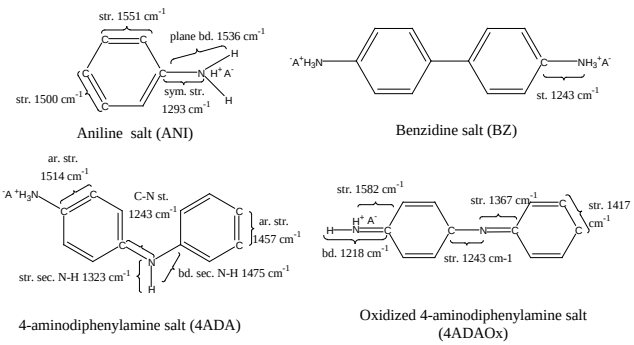

Scheme 2 . Vibrational band assignments for monomeric and dimeric species. The assignments are made by comparison with data from literature (see Table 1) and DFT calculations (see Table 1 and ESI). A^- are the anions present in the electrolyte (ClO_4^- in this work)

[⊗] Note that in ref. c the spectrum of adsorbed benzidine is described.

According to the spectra in Figure 1B, upon ANI oxidation a positive band appears at ca. 1500 cm^{-1} due to ANI consumption. However, in the same region during potential steps in the negative going direction, this signal diminishes probably due to the BZ production, which should absorb at 1501 cm^{-1}. Moreover, 4ADA is also generated in high amounts as it is shown in the growth of a negative band in the backward scan at ca. 1514 cm^{-1}, corresponding to this dimer.

Electrochemistry of the dimers

To check these ideas, the spectra of the dimers (Figure 2) were measured during oxidation in comparable conditions to those in Figure 1. It is noteworthy that 4ADA adsorbs on the Pt electrode, giving a CV with a peak at the same potential than the one of the adsorbate shown in Fig.3.A and does not desorb upon oxidation.

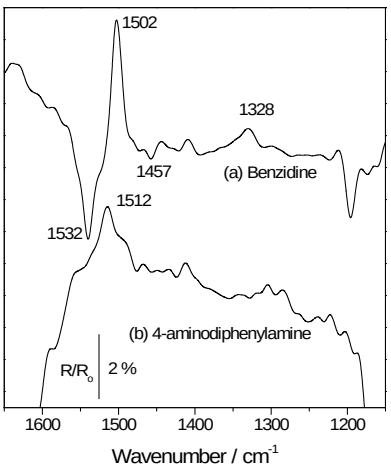

Figure 2. (a) In-situ FTIR difference spectrum taken during oxidation of BZ (10 mM/1 M $HClO_4$) at 1.0 V_{RHE} (0.1 V_{RHE} as reference). (b) In-situ FTIR difference spectrum taken during oxidation of 4ADA (10 mM/1 M $HClO_4$) at 0.8 V_{RHE} (0.1 V_{RHE} as reference). Spectra taken with p-polarized light, 128 scans at 8 cm^{-1} resolution.

As it can be seen, the oxidation of adsorbed 4ADA reveals a clear positive band at 1512 cm^{-1} related to its consumption, while the oxidation of BZ shows a positive consumption band at 1502 cm^{-1} and a negative band at 1532 cm^{-1}. The later is related to oxidized BZ and could be assigned to the imine bending of N-H (C=N-H). Therefore, it is spectroscopically demonstrated the formation of BZ and 4ADA during ANI oxidation.

A second point to be clarified is the presence of adsorbed species during the oxidation process. It has been usually assumed that only soluble intermediates and oligomers/polymers are formed. On the other hand, it has been proposed[47] that the head-to-tail dimer is adsorbed onto the electrode. To test that, we use a flow cell which allows solution exchange maintaining the potential control of the working electrode. First, the potential was stepped from 0.1 to 1.2 V_{RHE} and left for 2 min in a 10 mM ANI/1 M $HClO_4$ solution. Then, the potential was set at 0.1 V_{RHE} again and the solution exchanged with 10 times the cell content of monomer free electrolyte.

The CV acquired after that procedure (Figure 3A) shows clearly a quasi-reversible peak due to an adsorbed layer.[47] The peak position matches that of 4ADA produced during oxidation (see peak c-c` in Figure 1A). The FTIR spectrum of the oxidized dimer given in Figure 3B (taken at 0.8 V_{RHE} with 0.6 V_{RHE} as reference) display positive bands at 1511 and 1313 cm^{-1} and negative bands at 1582, 1417, 1367, 1243 and 1218 cm^{-1}. The spectrum is quite similar to the one of 4ADA taken in the same conditions. The band assignments are summarized in Table 2.

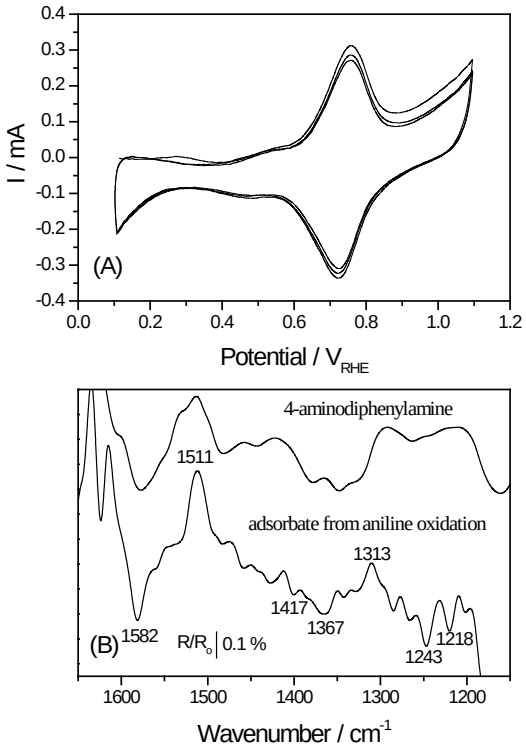

Figure 3. (A) CV of the adsorbate produced in the experiment described in Figure 1. Scan rate = 50 mV/s. (B) In-situ difference FTIR spectrum (taken at 0.8 V_{RHE} using 0.6 V_{RHE} as reference) of the adsorbate produced during ANI oxidation. The spectrum of 4ADA adsorbed from its solution in ethanol is shown for comparison. Spectra taken with p-polarized light, 128 scans at 8 cm^{-1} resolution.

PANI redox switching

The CV in 0.1 M $HClO_4$ of a thick PANI film synthesized from 0.1 M ANI/1 M $HClO_4$ solution is given in Figure 4A. As it can be seen, two redox couples are clearly detected which correspond to two reversible redox processes in the polymer. The mechanism of redox switching of PANI, coupled to anion and proton exchange, has been elucidated using a variety of in-situ techniques. [49] It could be described as in Scheme 3. It is noteworthy that the so called "middle peak" is absent in the CV shown in Figure 4A. This is due to the fact that relatively high aniline concentration (0.1 M) is used making favorauble the grow of the polymer chain and decreasing the amount of adsorbed 4ADA (see below). On the other hand, special care was taken to avoid high potentials (> 1.05 V_{RHE}) or high current densities (> 0.5 mA/cm^2), to avoid film degradation. In that way, complete depletion of aniline

from the diffusion layer is avoided. Otherwise, if aniline is depleted, the oxidized polymer could react with water leading to degradation (see below).

Table 2. Assignment of vibrational bands of the isolated adsorbate produced during ANI oxidation (Figure 3B). The wavenumber values calculated by DFT to the vibrations described in the table are shown between parentheses.

Wavenumber/ cm^{-1}	Sense	Vibration	Species
1582 (1590)	-	C=N str. [a]	*4ADAOx*
1511(1536)	+	C=C aromat. str. [b]	*4ADA*
1417 (1436)	-	C-C str. [c]	*4ADAOx*
1367 (1382)	-	C-N stretching in a quinonimine ring.[d]	*4ADAOx*
1313 (1309)	+	C-N stretching [b]	*4ADA*
1243 (1245)	-	C-N str. in C-N=C[e]	*4ADAOx*
1218 (1221)	-	-NH bend[c]	*4ADAOx*

[a] *S. Quillard, G. Louarn, J.P. Buisson, M. Boyer, S. Lefrant, M. Lapkowski, A. Pron,* Synth. Met., *1997, **84**, 805.*

[b] *P. Sett, A.K. De, S. Chattopadhyay, P.K. Mallick,* Chemical Physics, *2002, **276**, 211-224.*

[c] *E. Pretsch, P. Bühlmann, C. Affolder,* Structure Determination of Organic Compounds, *Springer, Berlin, 2000.*

[d] *L. Brožová, P. Holler, J. Kovářová, J. Stejskal, M. Trchová,* Polymer Degradation and Stability, *2008, **93,** 592-600.*

[e] *S. Quillard, G. Louarn. S. Lefrant, A.G. MacDiarmid,* Phys Rev B, *1994, **50**,12496-12508*

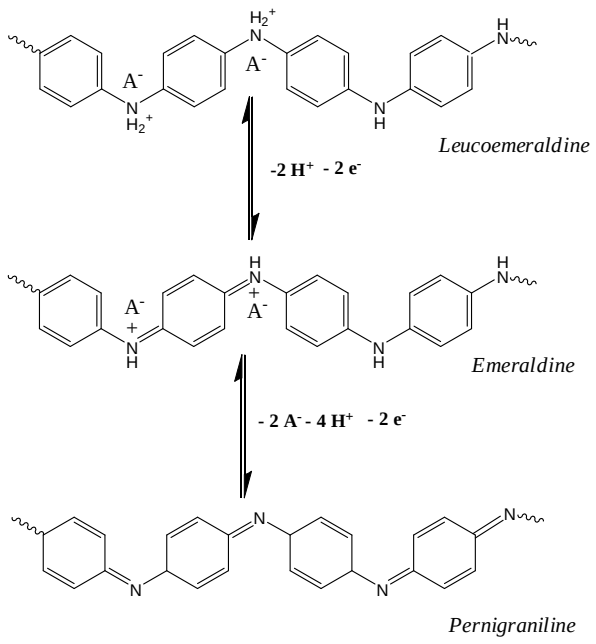

Scheme 3. Changes of chemical structures during oxidation/reduction of PANI in acid media. A^- are the anions present in the electrolyte (ClO_4^- in this work).

While different protonation states exist at different pH, the structures described are the more likely to exists at pH = 0. Accordingly, in the first oxidation step, anion insertion should take place to compensate for the positive charge formed inside the polymer. However, since the reduced state of the polymer is a polyamine, it is protonated at pH = 1. Therefore, the charge is finally compensated by proton expulsion. During the second oxidation step, protons and anions are expelled since the pernigraniline state (a quinonimine chain) is less basic and easily deprotonates.

Table 3. Assignment of vibrational bands observed during 0.05 and 0.1 M PANI oxidation (Figures 4 and 5). The wavenumber values calculated by DFT to the vibrations described in the tect are shown between parentheses.

Wavenumber/ cm^{-1}		Sense	Vibration[a]	Species[&]
P005[#]	P01[#]			
1581 (1588)	1581	-	N=Q=N* str.[b]	*EM*
1512 (1546)	1512	+	C=C aromat. str. N-B-N	*LE*
1475 (1462)	1487	-	C=C aromat. str. N-B-N	*PN*
1450 (1422)	-	-	C=C aromat. str. N-B-N	*PN*
1423 (1433)	-	+	C-N str.	*LE*
1377 (1381)	1360	-	C-N str.[c]	*EM and PN*
1342 (1309)	-	-	C-C str., N-H o.o.p. bend	*EM*
1288 (1277)		+	C–N str. sec. aromatic amine[d]	*LE*
1238	1268	-	C-N stretch, C-C-C ring i.p. def.	*EM*
1218 (1213)	-	+	$-NH_2^+$ bend.	*LE*
1157 (1154)	1189	-	N=Q=N[e] C-H in plane bending[c]	*EM*

[*] *Q = quinonoid unit, B= benzenoid unit,*

[&] *LE = leucoemeraldine unit, EM = emeraldine unit, PN = pernigraniline unit*

[#] *P005= PANI produced in 0.05 M ANI, P01 = PANI produced in 0.1 M ANI*

[a] *E.P. Pretsch, P. Bühlmann, C. Affolder,* Structure Determination of Organic Compounds, *Springer, Berlin, 2000.*

[b] *C. Yang, C. Chen, Y. Zeng,* Spectrochimica Acta Part A: Molecular and Biomolecular Spectroscopy, *2007, **66**,37-41.*

[c] *L. Brožová, P. Holler, J. Kovářová, J. Stejskal, M. Trchová,* Polymer Degradation and Stability, *2008, **93**, 592-600.*

[d] *S. Kazim, V. Ali, M. Zulfequar, M. Mazharul Haq, M. Husai,* Current Applied Physics, *2007, **7,** 68-75.*

[e] *R. Singh, V. Arora, R.P. Tandon, S. Chandra, N. Kumar, A. Mansingh,* Polymer, *1997, **38**, 4897.*

Although the infrared spectra of thick PANI films obtained from electropolymerization in solutions with ANI content equal or higher than 0.1 M have been extensively reported in the literature [23-30], there are different explanations for similar bands. The characterization of the vibrational modes is difficult due to the baseline shift related with the change from a non conductive polymer (leucoemeraldine form) to a conductive one (emeraldine form). Complete assignment of the bands requires additional data, such as isotope exchange in

the electrolyte and monomer, which is out of the scope of the present paper. However, a tentative assignment is made in Table 3, in analogy with the band interpretation made in the spectra of thin PANI films (produced in a 0.05 M ANI solution) discussed later.

A typical spectrum of a film produced by electropolymerization from a 0.1 M ANI solution in 1 M $HClO_4$ is shown in Figure 4B.

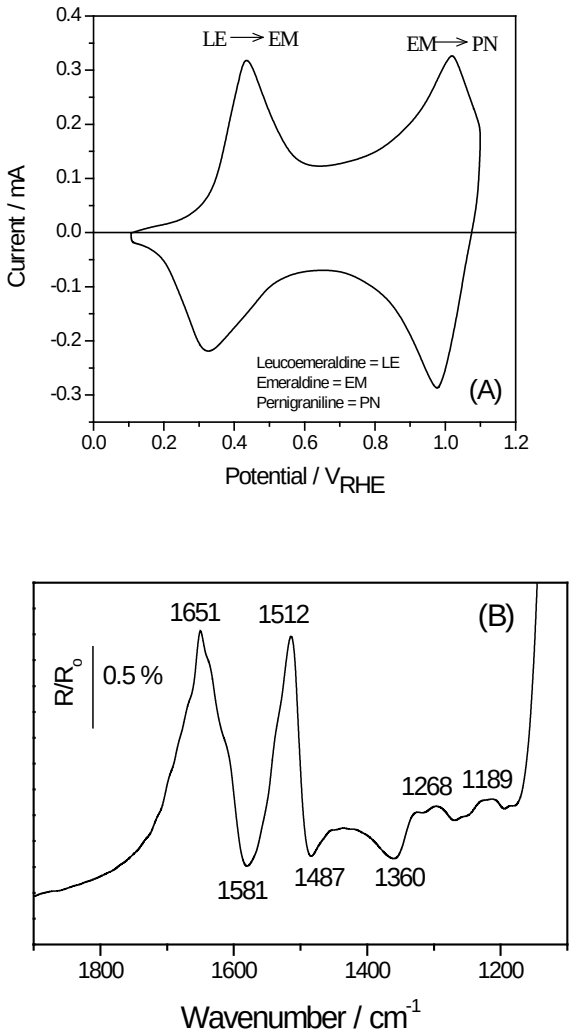

Figure 4. (A) CV of a thick (> 150 nm) PANI film in 1 M $HClO_4$. Scan rate = 50 mV/s. (B) Corresponding in-situ FTIR spectrum taken at 0.8 V_{RHE} (reference taken at 0.1 V_{RHE}). Spectrum taken with p-polarized light, 128 scans at 8 cm^{-1} resolution.

Figure 5A shows the CV of a thin PANI film produced in 0.05 M ANI/0.1 M $HClO_4$. The response displays two broad redox processes and, as a difference with Figure 4A, a clear middle peak. The question remains if the "middle peak" is due to degradation products (e.g. quinones) or to adsorbed 4ADA. The FTIR spectra of the thin film are shown in Figure 5B.

It is noteworthy that the spectra develop a constant baseline allowing assignment of positive and negative bands, in contrast with thick PANI films in Figure 4B (made in 0.1 M ANI solution), which show a drift of the baseline due to the development of free carrier absorption in the film, linked to the polymer conductivity.

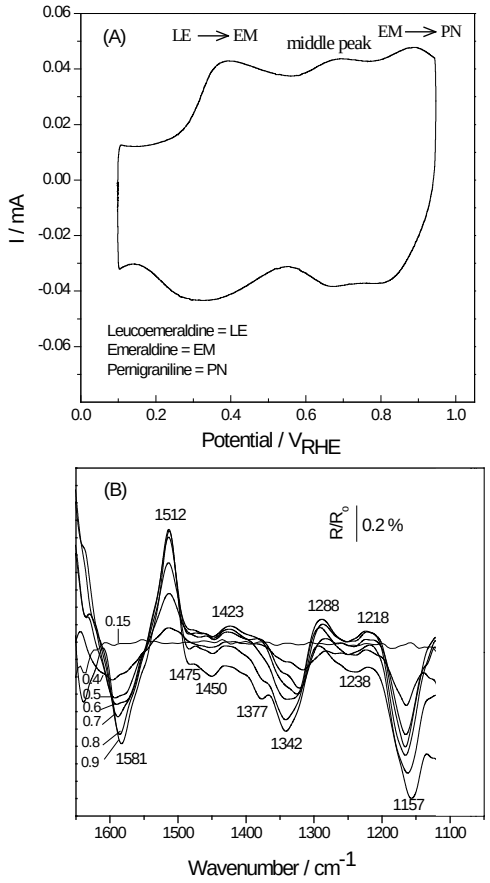

Figure 5. (A) CV of the polymer obtained by oxidation of a 0.05 mM ANI/0.1 M $HClO_4$ solution on polycrystalline Pt. San rate = 50 mV/s. (B) Corresponding in-situ FTIR spectra acquired during oxidation of the polymer (reference spectrum taken at 0.1 V_{RHE}). Spectra taken with p-polarized light, 128 scans at 8 cm^{-1} resolution. Sample potentials as indicated in the Figure.

The band assignments are summarized in Table 3 and Scheme 4. The signal at 1512 cm^{-1}, associated with C=C stretching of the amine aromatic rings, increases intensity upon oxidation due to the consumption of amine aromatic rings in the conversion from leucomeraldine to emeraldine state (Scheme 3). Accordingly, the band at 1581 cm^{-1}, assigned to C=N and C=C stretching in the quinonimine units, increases intensity upon oxidation due to the formation of quinonimine units in the emeraldine state. The feature at 1157 cm^{-1} assigned to imine (C=N-H) vibrations also increases due to an increased quinonimine content in the oxidized film.

It can be seen that there are signals which appear as doublets in Figure 5B (1475 and 1450 cm^{-1}, 1377 and 1342 cm^{-1}). Such bands are present in the spectrum of thick PANI as single bands (Figure 4B). It seems that similar vibrations exist in the dimer (4ADA) and the polymer albeit with different energies. This is likely to be due to the effect of extended delocalization

of charge in the polymer which broadens the bands; such effect does not exist in the dimer 4ADA. On the other hand, several bands observed in the thin film have analogous bands in the thick film (see Table 3 and Scheme 4). The results confirm that ANI concentration plays a major role on the products obtained by electropolymerization. While a conductive PANI film relatively free of 4ADA is obtained at higher concentrations of the monomer (0.1 M), a film rich in 4ADA is obtained at lower concentrations, as clearly depicted by the "middle peak" in the CV in Figure 5A.

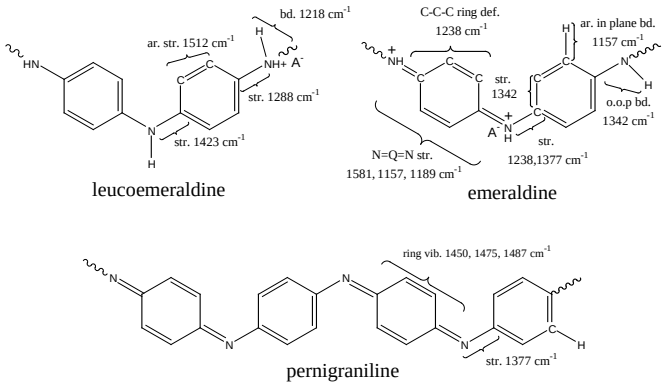

Scheme 4. Vibrational band assignments for polymeric species. The assignments are made by comparison with data from literature (see Table 3) and DFT calculations (see Table 3 and ESI). A^- are the anions present in the electrolyte (ClO_4^- in this work).

Therefore the main difference between the films produced in 0.1 M and 0.05 M ANI concentration is the relative amount of adsorbed 4ADA to PANI.

PANI degradation

By subjecting the polymer to a potential higher than ca. 0.80 V_{RHE} in acid aqueous media, the polymer suffers degradation. To study that process by FTIRS, a PANI film produced by electropolymerization of a 0.1 M ANI solution in 1 M $HClO_4$ (thick film) was subsequently potentiostatized at 1.1 V_{RHE} in a monomer free 0.1 M $HClO_4$ solution for 400 s.

The CV of the degraded film (Figure 6A) shows a clear "middle peak" at ca. 0.65 V_{RHE} after the potentiostatic treatment. At potentials more positive than 0.80 V_{RHE}, the film is in its fully oxidized form (pernigraniline), which is highly reactive to nucleophilic attack. [50] In a monomer free aqueous solution the best nucleophile is water, which could attack the imine nitrogen, breaking the polymer chain and producing ammonium ion and p-benzoquinone as soluble products (Scheme 5). [51] The latter is reduced to hydroquinone when the electrode potential is stepped back to 0.1 V_{RHE}. To check if this reaction occurs, the spectrum of the solution was taken after degradation (measured at 0.8 V_{RHE} after reduction at 0.1 V_{RHE}, where the reference spectrum is measured) and compared with a spectrum of a solution of hydroquinone subjected to the same potentials (Figure 6B).

The spectrum obtained during oxidation of hydroquinone (dashed line) agrees with previous reports. [52] The results are summarized in Table 4.

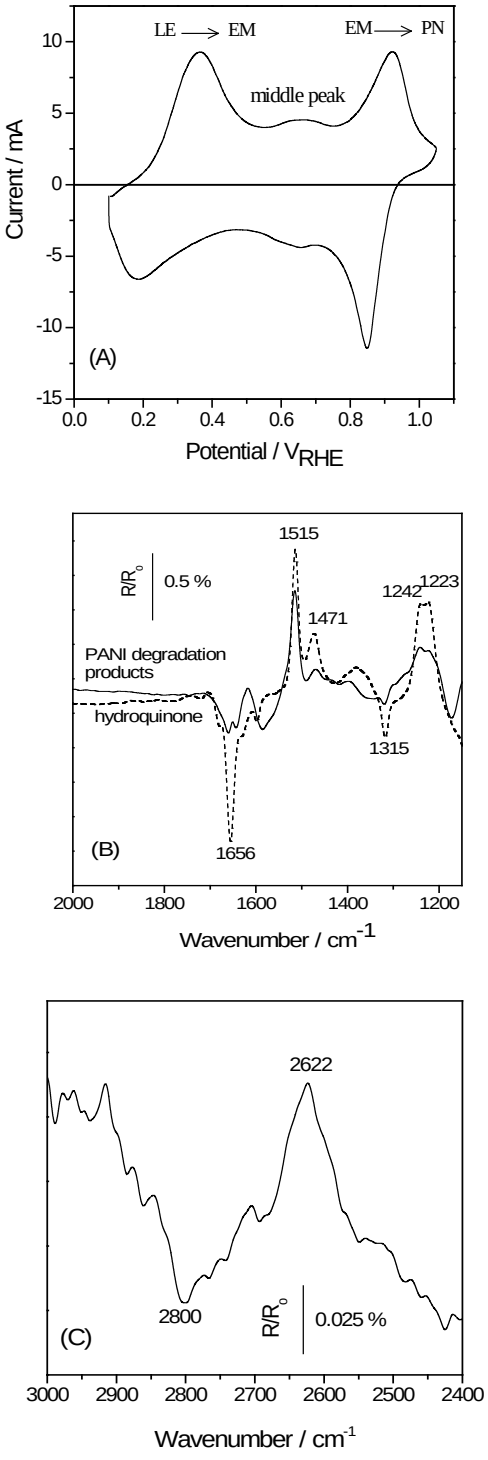

Figure 6. (A) CV of a PANI film in 1 M $HClO_4$ after potentiostatic degradation (50 sec. at 1.1 V_{RHE} in 0.1 M $HClO_4$). Scan rate = 50 mV/s. (B) Corresponding in-situ FTIR spectrum (solid line) for degraded PANI in the region 2000-1100 cm^{-1}. For comparison, the FTIR spectrum taken at 0.8 V_{RHE} (reference taken at 0.1 V_{RHE}) during oxidation of hydroquinone (10 mM/1 M $HClO_4$) on polycrystalline Pt is shown. Spectra taken with p-polarized light, 128 scans at 8 cm^{-1} resolution. (C) Same as (B) solid line but in the region 3000-2400 cm^{-1}.

Table 4. Assignment of vibrational bands observed after degradation of PANI and its comparison with hydroquinone. (Figure 6). The wavenumber values calculated by DFT to the vibrations described in the table are shown between parentheses.

Wavenumber/ cm^{-1}	Sense	Vibration[a]	Species[&]
2800[a] (2795)	-		*IN*
2622[a] (2618)	+		*IN*
2340[a] (2345)	-	asym. str.	CO_2
1656[b] (1654)	-	C=O stretching	*BQ*
1515[c] (1518)	+	C=C ar. str.	*HQ*
1471 (1426)	+		*HQ*
1315 (1309)	-		*BQ*
1242[d] (1237)	+	C-O-H sym. str.	*HQ*
1223[d] (1225)	+	C-O-H asym. str.	*HQ*

[&] *HQ = hydroquinone, BQ = benzoquinone, IN= indophenol.*

[a] *E.P. Pretsch, P. Bühlmann, C. Affolder,* Structure Determination of Organic Compounds, *Springer, Berlin, 2000.*

b D. Lin-Vien, N.B. Colthup, W.G. Fateley, J.G. Grasselli, The Handbook of Infrared and Raman Characteristic Frequencies of Organic Molecules, *Academic Press, San Diego, USA, 1991.*

c G. Sócrates, Infrared Characteristic Group Frequencies, *Wiley, New Cork, 1980.*

d L.J. Bellamy, Advances in infrared group frequencies, *Halsted Press, London, 1975.*

In this spectrum, positive bands are related to the consumption of hydroquinone and negative bands to the production of benzoquinone. Thus, the positive band at 1515 cm^{-1} is assigned to C=C aromatic stretching of hydroquinone,[53] whereas the negative feature at 1656 cm^{-1} is due to the C=O stretching of benzoquinone.[54] Accordingly, the positive bands at 1242 and 1223 cm^{-1}, are related to the symmetric and asymmetric stretching of C-O-H in the hydroquinone.[55] Finally, the negative band at 1315 cm^{-1}, assigned to the C=C-C=O stretching in benzoquinone, increases intensity upon benzoquinone production. Comparing both spectra in Figure 6B, it can be concluded that most bands are coincident, supporting the assignment of p-benzoquinone as the main product of PANI degradation.

It is obvious that the nature of the "middle peak" observed here (Figure 6A) is different than the one observed during polymerization (Figure 5A). During degradation, benzoquinone is produced and retained inside the polymer. During polymerization, 4ADA is produced and adsorbed on the electrode surface. While the voltammetric profile does not allow distinguishing between both species, FTIRS clearly show that they are different. Thus, a positive band appears at 2622 cm^{-1} while a negative feature is present at 2800 cm^{-1} (Figure 6C). The contribution at ca. 2622 cm^{-1}, previously assigned to charged amino groups (see ANI oxidation section), increases its intensity during oxidation and decreases during reduction (not shown). This behaviour suggests that other species, like indophenol (see Scheme 3), are also present in the solution after degradation. The band is absent in the spectra taken during redox switching of PANI, excluding vibrations in the polymer to explain the band.

A band at 2340 cm^{-1} (not shown) which increases intensity during oxidation and remains constant during reduction is observed in the spectra. This feature confirms that also CO_2 is produced during degradation of PANI films on Pt by complete oxidation of the ANI aromatic rings. This is quite relevant because it is likely that polymer complete oxidation to CO_2 will occur at the Pt/PANI interface since Pt is necessary to break the C-H bonds. Therefore, by subjecting a PANI/Pt film to a potential higher than ca. 0.8 V_{RHE}, it is possible to produce a PANI film which seems unaltered but have an interlayer of degraded polymer. The electronic conduction of such film at high frequencies will be highly impaired.

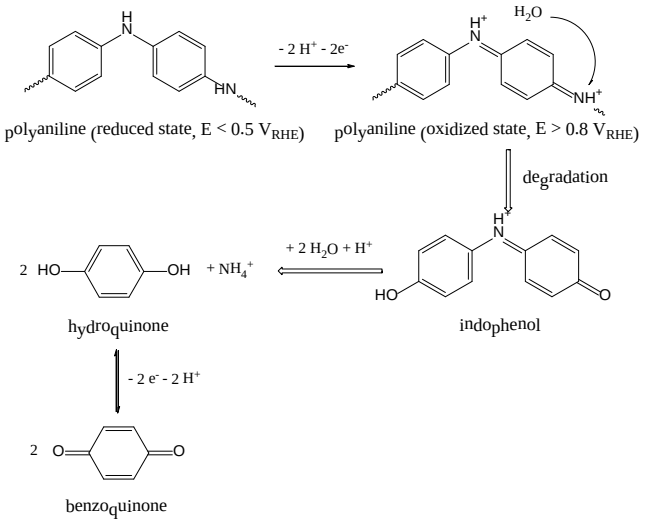

Scheme 5. Reactions occurring during the electrochemically promoted degradation

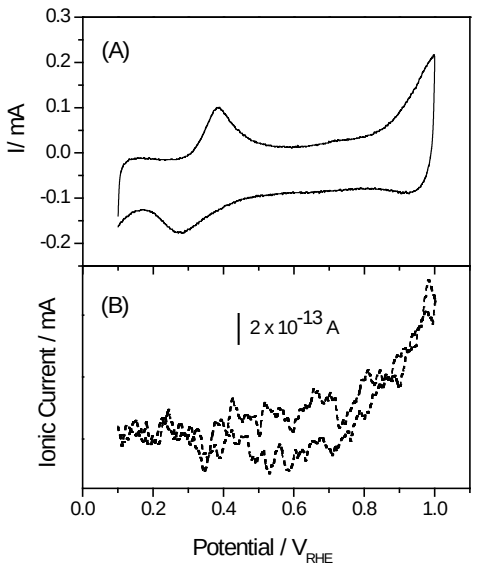

Figure 7 Electrochemically promoted degradation of a PANI film in 0.1 M $HClO_4$. (A) CV obtained during PANI degradation onto a porous Pt electrode. Scan rate = 10 mV/s. (B) Corresponding MSCV for CO_2 (m/z = 44).

To test that hypothesis, DEMS was used to study the formation of volatile species. As is can be seen in Figure 7, CO_2 is produced when a PANI film is subjected to potential excursions beyond 0.8 V_{RHE}. An interesting result is that PANI can be completely burn out of a Pt electrode, effectively

cleaning the electrode, by scanning between 0 a 1.5 V_{RHE} in acid solution.

Conclusions

In the present work, three main conclusions could be drawn. First, that the spectroscopic evidences obtained support the ANI electroxidation mechanism proposed by Bacon & Adams.[15] The early stages of ANI seem to involve monomer oxidation to its cation radical, which dimerizes. Two dimers are produced by head-to-tail and tail-to-tail coupling. The FTIR study shows evidence of the formation and oxidation/reduction of both dimers. It is found that the head-to-tail dimer (4ADA) is adsorbed in the electrode surface, giving rise to the "middle peak" observed after polymerization in the CV of PANI. The feature is more clearly detected in polymer films produced at low ANI concentrations, suggesting that 4ADA rich films are produced in those conditions. On the other hand, the tail-to-tail dimer (BZ) remains in solution. It is therefore more likely for PANI chains to be initiated by 4ADA units than BZ units. Since 4ADA is adsorbed, the magnitud of the current associated to the "middle peak" is related to the relative amount adsorbed 4ADA and polyaniline.

Secondly, the redox switching of PANI is clearly shown to involve oxidation of amine units to quinonimine units. The bands due to polymer oxidation/reduction are more clearly observed in thin polymer films, where the disturbance of shifting baseline due to changes in polymer conduction bands is not present.

Finally, during degradation of PANI, benzoquinone is produced by nucleophilic attack of water on the fully oxidized polymer. This gives rise to a "middle peak" in the CV of PANI after degradation with different nature to the "middle peak" observed after polymerization. Therefore the nature of the same voltammetric feature depends on the source of the chemical species. In thin films of PANI, produced at aniline concentrations below 0.1 M, the "middle peak" is related to the redox response of 4ADA adsorbed onto the electrode. On the other hand, if thick PANI films, where no such peak is observed (see Fig. 4A), are subjected to electrochemical degradation by oxidation to its pernigraniline state in acid solution, a different species is produced: benzoquinone which is oxidized/reduced in the same potential region. Obviously, if the polymerization is carried out at too high potentials or current densities, the monomer concentration decreases to zero in front of the electrode. Therefore, the film degrades during polymerization and a mixture of adosrbed 4ADA and benzoquinone could be related to the presence of the "middle peak" feature.

During degradation of PANI, other bands assigned to indophenol are also observed. Additionally, CO_2 is detected by in-situ FTIR and DEMS during formation and degradation of PANI. This means that the polymer could be electrochemically burned on the Pt surface. On one hand, such process could be used to completely clean off Pt electrode surfaces covered with PANI. On the other hand, it means that extreme care should be taken with the potentials applied to Pt electrodes covered by PANI films to avoid electronic disconnection (or high resistance barriers) of the polymer layer from the base metal. In the best of our knowledge, this is the first evidence of the oxidation of a conducting polymer to CO_2 by electrochemical means.

In-situ external reflection FTIR proves to be an excellent method to investigate early stages of conductive polymer formation, because it allows positive identification of chemical species produced/consumed during electrochemical reactions. It also allows finding out previously undetected species (e.g. indophenol, CO_2) or differentiate between species (adsorbed 4ADA, benzoquinone) which has similar oxidation/reduction behaviour making it impossible by cyclic voltammetry.

C.A.B. and G.A.P. are permanent research fellows of CONICET. The work was financed by MCYT (MAT2008-0xxx-CO3-02, Spain) and SECYT-UNRC (PDMA), CONICET (PIP5201), FONCYT (PICTR03-453), ARGENTINA). The authors acknowledged the financing by AECI of the collaboration project (PCI A/4233/05, A/5301/06 and xxxxx).

Notes and references

[a] *Dpto. de Química Física, Universidad de la Laguna, 38071 –Tenerife Spain. Fax: +34-922318002;Tel: +34-922318028; E-mail: epastor@ull.es*

[b] *Dpto de Química, Universidad Nacional de Río Cuarto, 5800- Río Cuarto, Argentina.*

† Electronic Supplementary Information (ESI) available: figures of simulation and additional experimental data

1 H.S. Nalwa, Ed, *Handbook of Organic Conductive Molecules and Polymers, Conductive Polymers: Spectroscopy and Physical Properties*, John Wiley & Sons, New York, 1997

2 A.G. MacDiarmid, A.J. Epstein, *Faraday Discuss. Chem. Soc.*, 1989, **88**, 317

3 R.N. Adams, *Electrochemistry at solid electrodes*, Marcel Dekker, New York, 1969, pp 331.

4 L.D. Claxton, T.J. Hughes, K-T. Chung, Food and Chem. Toxic., 2001, **39**, 1253

5 E.M. Geniès, A. Boyle, M. Lapkowski, C. Tsintavis, *Synth. Met.*, 1990, **36**, 139

6 D. Li, R.B. Kaner, *J. Am. Chem. Soc.*, 2006**, 128**, 968.

7 a) L. Duic, M. Kraljic, S. Grigic, *J. Pol. Sci. A: Pol. Chem.*, 2004, **42**, 1599; b) C. Mailhe-Randolph, A.J. McEvoy, *Ber. Bunsen-Ges. Phys. Chem*, .1989, **93**, 905.

8 Y. Wei, G.W. Jang, C.C. Chan, K.F. Hsueh, S. Hariharan, R.A. Patel, C.K. Whitecar, *J. Phys. Chem.*, 1990, **94**, 7716.

9 K. Tzou, R.V. Gregory, *Synth. Met.* 1992, **47**, 267.

10 Y. Wei, Y. Sun, X. Tang, *J. Phys. Chem.*, 1989, **93**, 4878.

11 J.C. Michaelson, A.J. McEvoy, N. Kuramoto, *J. Electroanal.l Chem.* 1990, **287**, 191; G.M. Morales, M.C. Miras, C. Barbero, *Synth. Met.*, 1999, **101**,686.

12 a) C. Mailhe-Randolph, J. Desilvestro, *J. Electroanal. Chem.* 1989, **262**, 289; b) G. Zotti, S. Catarin, N. Comisso., *J. Electroanal. Chem.*, 1988, **239**, 387.

13 H. Yang, A.J. Bard, *J. Electroanal. Chem.*, 1992, **339**, 423 and references therein

14 A. Malinausakas, *Synth. Met.*, 1999,**107**,75.

15 J. Bacon, R.N. Adams, *J. Amer. Chem. Soc.*, 1968, **90**, 6596.

16 S-Y Hong, Y.M. Jung, S.B. Kim, and S-M Park. *J. Phys. Chem. B* 2005, **109**, 3844.

17 T. Iwasita, F.C Nart in Advances in *Electrochemical Science and Engineering*, Gerischer, H. and Tobias, C.W. (Eds), VCH, Weinheim, 1995.

18 a) D. Kolbe, W. Vielstich, Electrochim. Acta, 1996, **41**, 2457; b) R. Ianniello, V.M. Schmidt, U. Stimming, J. Stumper, A. Wallau, *Electrochim. Acta*, 1994, **39**, 1863.

19 a) V.M. Schmidt, J. Stumper, E. Pastor, J. Schmidberger, A. Hamelin, *Surf. Science*, 1995, **335**, 197; b) J.L. Rodriguez, E. Pastor, X.H. Xia, T. Iwasita, *Langmuir*, 2000, **16**, 5479.

20 a) Z. Ping, G.E. Nauer, H. Neugebauer, J. Theiner, *J. Electroanal. Chem.*, 1997, **420**, 301; b) Z. Ping, G.E. Nauer, H. Neugebauer, J. Theiner, A. Neckel, *Electrochim. Acta*, 1997, **42**, 1693; Z. Ping, G.E. Nauer, H., Neugebauer, A. Neckel, *Electrochim. Acta*, 1996, **41**, 767; Z. Ping, G.E. Nauer, H. Neugebauer, A.Neckel, *Synth. Met.*, 1995, **69**, 161.

21 H. Neugebauer, A. Neckel, N.S. Sariciftci, H. Kuzmany, *Synth. Met.*, 1989, **29**, 185.

22 N.S. Sariciftci, M. Bartonek, H. Kuzmany, H. Neugebauer, A. Neckel, *Synth. Met.*, 1989, **29,** 193.

23 V.W. Jones, M. Kalaji, G. Walker, C. Barbero, R. Kötz, *J. Chem. Soc. Farad. Trans.*, 1994, **90**, 2061.

24 K. Ogura, K. Nakaoka, M. Nakayama, *J. Electroanal. Chem.*, 2000, **486**, 119.

25 M. Nakayama, M. Iino, K. Ogura, *J. Electroanal. Chem.*, 1997, **440**, 125.

26 A. Zimmermann, U. Künzelmann, L. Dunsch, *Synth. Met.*, 1998, **93**, 17.

27 P. Rapta, R. Fáber, L. Dunsch, A. Neudeck, O. Nuyken, *Spectrochim. Acta, A* 2000, **56,** 357.

28 A. Petr, L. Dunsch, *J. Electroanal. Chem.*, 1996, **419**, 55.

29 M. Nakayama, S. Saeki, K. Ogura, *Anal. Sci*., 1999, **15,** 259.

30 S. Quillard, G. Louarn, J. P. Buisson, M. Boyer; S. Lefrant, M. Lapkowski, A. Pron, *Synth. Met.*, 1997, **84**, 805.

31 T. Lindfors, C. Kvarnström, A. Ivaska, *J. Electroanal. Chem.*, 2002, **518**, 131.

32 M-C. Bernard, C. Deslouis, T. El Moustafid, ; A. Hugot-LeGoff, S. Joiret, B. Tribollet, *Synth. Met.*, 1999, **102**, 1381.

33 J.E. Pereira Da Silva, S.I. Córdoba De Torresi, D.L.A. De Faria, M.L.A. Temperini, *Synth. Met*., 1999, **101,** 834.

34 M. Baibarac, L. Mihut, I. Baltog, M. Cochet, S. Lefrant M. Lapkowski, *Synth. Met.*, 1998, **96,** 63.

35 A. Malinauskas, M. Bron, R. Holze, *Synth. Met.* 1998, **92**, 127.

36 R. Holze, *J. Electroanal. Chem.*, 1988, **250**, 145.

37 U. Schmiemann, Z. Jusys, H. Baltruschat, *Electrochim. Acta*, 1994, **39**, 561.

38 F. Cases, F. Huerta, P. Garcés, E. Morallón, J.L. Vázquez, *J. Electroanal. Chem.*, 2001, **501,** 186.

39 F. Cases, F. Huerta, R. Lapuente, C. Quijada, E. Morallón J.L. Vázquez, *J. Electroanal. Chem.*, 2002, **529**, 59.

40 R. Mazeikienè, A. Malinauskas, *Synth. Met.*, 2001, **123,** 349 and refs therein.

41 G. Zotti, S. Cattarin, N. Comisso, *J. Electroanal. Chem.*, 1987, **235**, 259.

42 E.M. Genies, M. Lapkowski, J.F. Penneau, *J. Electroanal. Chem.*, 1988, **249**, 97

43 S. Golczak, A. Kanciurzewska, M. Fahlman, K. Langer, J.J. Langer. *Solid State Ionics* 2008, **179,** 2234.

44 G.A. Planes, E. Moran, J.L.Rodriguez, C. Barbero, E. Pastor, *Langmuir*, 2003, **19**, 8899.

45 H. Baltruschat, U. Müller, U. Schmiemann, A. Dülberg, *Surf. Sci.*, 1995, **335**, 333.

46 SDBSWeb: http://www.aist.go.jp/RIODB/SDBS/ (14-Aug-2008)

47 L. Duic, Z. Mandil, S. Kovac, *Electrochim. Acta*, 1995, **40**, 1681.

48 A.J. Bard, L.R. Faulkner, *Electrochemical methods, Fundamentals and applications*, 2nd Ed, J. Wiley & Sons, New York, 2001, pp 591.

49 R.L. Hand, R.F. Nelson, *J. Am. Chem. Soc.*, 1974, **96**, 850.

50 C. Barbero, M.C. Miras, O. Haas, R. Kötz, *J. Electrochem. Soc.*, 1991, **138**, 669 and refs therein.

51 a) H. Salavagione, G.M. Morales, M.C. Miras, C. Barbero, *Acta Polym.*, 1999, **50,** 40; b) D.E. Grumelli, E.S. Forzani, G. M. Morales, M. C. Miras, C.A. Barbero, E.J. Calvo, *Langmuir*, 2004, **20**, 2349.

52 a) D. Orata, D.A. Buttry, J. Am. Chem. Soc., 1987, **109,** 3574; b) X. Yang, Q. Xie, S. Yao, *Synth. Met.* 2004, **143**, 119; c) R. Mazeikiene, A. Malinauskas, *Eur. Polym. J.*, 2002, **38**, 1947.

53 C.F. Zinola, J.L. Rodríguez, M.C. Arevalo, E. Pastor, *J. Electroanal.* Chem., 2005, **585**, 230.

54 G. Sócrates, *Infrared Characteristic Group Frequencies*, Wiley, New Cork, 1980.

55 D. Lin-Vien, N.B. Colthup, W.G. Fateley, J.G. Grasselli, *The Handbook of Infrared and Raman Characteristic Frequencies of Organic Molecules*, Academic Press, San Diego, USA, 1991.

55 L.J. Bellamy, *Advances in infrared group frequencies*, Halsted Press, London, 1975.